

Predicting adsorption isotherms using a two-dimensional statistical associating fluid theory

Alejandro Martinez and Martin Castro

Instituto de Fisica, Universidad de Guanajuato, Lomas del Bosque 103, Colonia Lomas del Campestre, Leon 37150, Mexico

Clare McCabe

Department of Chemical Engineering, Vanderbilt University, Nashville, Tennessee 37235-1604

Alejandro Gil-Villegas^{a)}

Instituto de Fisica, Universidad de Guanajuato, Lomas del Bosque 103, Colonia Lomas del Campestre, Leon 37150, Mexico

(Received 10 November 2006; accepted 11 January 2007; published online 21 February 2007)

A molecular thermodynamics approach is developed in order to describe the adsorption of fluids on solid surfaces. The new theory is based on the statistical associating fluid theory for potentials of variable range [A. Gil-Villegas *et al.*, *J. Chem. Phys.* **106**, 4168 (1997)] and uses a quasi-two-dimensional approximation to describe the properties of adsorbed fluids. The theory is tested against Gibbs ensemble Monte Carlo simulations and excellent agreement with the theoretical predictions is achieved. Additionally the authors use the new approach to describe the adsorption isotherms for nitrogen and methane on dry activated carbon. © 2007 American Institute of Physics. [DOI: 10.1063/1.2483505]

I. INTRODUCTION

Confined fluids are ubiquitous in chemical, geological, and biological processes and systems, for example, in the development of functionalized nanoporous adsorbents for environmental remediation¹ and nanoporous materials to separate contaminants from waste streams,² in releasing the oil trapped in pores during enhanced oil recovery, in biochemical separations using biomolecules in narrow pores,³ and in membrane transport through ion channels. Molecules confined within narrow pores exhibit physical behavior that can be significantly different from that observed in the bulk, as the introduction of surface forces and the competition between surface-wall and fluid-fluid interactions can lead to new kinds of phase changes not observed in the bulk.⁴ Of particular relevance are the confined fluids created by the selective adsorption of water, oil, gas, and enhanced oil recovery (EOR) fluids into the pores present in soil and rocks, and the phase transitions in these confined fluids. Hence, to improve the efficiency of EOR processes, a fundamental understanding of the phase behavior of confined fluids is needed.

Confinement effects can be taken into account by modeling fluids in the presence of an external potential due to the molecules forming the internal surface of the confining pores, or “wall.” As a consequence of this external interaction the fluid molecules adsorb onto the surface of the wall and changes in the thermodynamic properties of the fluid near the wall are observed in comparison with their bulk values, under the same conditions. The density of the fluid

near the wall becomes a function of the normal distance between the center of mass of a molecule and the wall, say, z . This introduces an inhomogeneity in the density and consequently other thermodynamic properties that are functions of the density also become z dependent. This local density naturally tends to the bulk value (independent of z) as we move further away from the wall.

Theoretical approaches to inhomogeneous fluids fall into two broad categories: density functional theory (DFT) and integral equation theories. DFT, in which the thermodynamic properties are expressed as functionals of the spatially varying single particle density, is perhaps the most widely used theory of inhomogeneous fluids.⁵ Integral equation theories have proven useful for studying the structure of confined fluids, though the description of phase changes has proven more difficult. The DFT approach to adsorption was proposed by Ebner *et al.*⁶ by minimization of the grand potential $\Omega = -PV$, where P is the pressure and V the volume of a fluid with a characteristic inhomogeneous density $\rho(\mathbf{r})$. The grand potential can be written as

$$\Omega = A(\rho(\mathbf{r})) + \int d\mathbf{r} \rho(\mathbf{r}) [w(\mathbf{r}) - \mu], \quad (1)$$

where A is the Helmholtz free energy in the absence of an external field, w the external field due to the pore material, and μ the chemical potential. This approach has been widely used to characterize the behavior of confined fluids, such as adsorption phenomena and capillary condensation in pores.^{7–12}

Over the last decade, the statistical associating fluid theory (SAFT),^{13,14} based on the thermodynamic perturbation theory for fluids with highly anisotropic interactions developed by Wertheim,^{15–20} has been extensively used to cal-

^{a)} Author to whom correspondence should be addressed. Electronic mail: gil@fisica.ugto.mx

culate the phase behavior of associating and nonassociating fluid systems. The SAFT approach has proven to be a powerful molecular based equation of state and has been applied to a wide variety of complex and industrially relevant fluid systems. Due to its predictive accuracy and versatility, the SAFT approach is rapidly superseding well established chemical engineering equations of state. Over the years several variations of the theory that have been proposed have improved the scope of application and predictive power of the method, including several SAFT-DFT approaches to study the liquid-vapor interface and confinement properties of associating fluids.^{21–26} See Refs. 27–30 for reviews on the SAFT approach.

In this work we broaden the scope of the statistical associating fluid theory for potentials of variable range³¹ (SAFT-VR) to describe the adsorption of chain molecules, based on a quasi-two-dimensional approach to describe the adsorbed fluid. In the spirit of the original SAFT-VR approach the theory developed is general in that different types of particle-particle and particle-wall potential models can be used. In this paper we present results for nonassociating chain molecules formed from spherical segments interacting via a square-well potential adsorbing on a uniform structureless wall. Results for a series of model fluids in comparison with computer simulation data are presented in order to validate the theory which is then applied to model the adsorption isotherms of methane and nitrogen on dry activated carbon.

II. THEORY

Previous studies on theoretical modeling of the adsorption of noble gases and other substances on structureless surfaces have been developed on the basis of mean-field theories in conjunction with a quasi-two dimensional approach.^{32–34} In this work we go beyond the mean-field approach by using the SAFT framework combined with perturbation theories for simple fluids. We first present the theory for the adsorption of monomer fluids and then consider chain fluids before summarizing the main expressions used in the SAFT-VR approach to describe the two-dimensional (2D) and three-dimensional (3D) fluids.

A. Adsorption of monomeric fluids

The model that we consider is a single-component fluid in the presence of a uniform wall. The fluid consists of N spherical particles of diameter σ . Due to the wall, the behavior of the particles is different depending upon their distance to the wall. The interaction exerted by the wall on a particle is given by

$$u_{pw}(z; \sigma, \lambda_w, \epsilon_w) = \begin{cases} \infty & \text{if } z \leq 0 \\ -\epsilon_w & \text{if } 0 < z \leq \lambda_w \sigma \\ 0 & \text{if } z > \lambda_w \sigma, \end{cases} \quad (2)$$

where z is the perpendicular distance of the particles from the wall, ϵ_w is depth, and $\lambda_w \sigma$ is the range of the attractive potential. Hence we can describe the system as being composed of two subsystems: a fluid whose particles are near to the wall, i.e., when $z \leq \lambda_w \sigma$, which we shall refer to as the “adsorbed fluid,” and a fluid whose particles are far from the

wall, i.e., when $z > \lambda_w \sigma$, i.e., the “bulk fluid.” In this way the length scale that characterizes the adsorbed fluid is given by $\lambda_w \sigma$. This approach is formally valid if we do not take into account the interface between the adsorbed and bulk fluids.

The adsorbed and bulk fluids have different properties due to the wall; it is well known that the interaction between molecules is modified by the presence of the wall and therefore the pair interaction between particles is different for the adsorbed and bulk phases.^{35,36} We denote $u_{pp}(r; \epsilon, \lambda)$ and $u_{pp}^{\text{ads}}(r; \epsilon_{\text{ads}}, \lambda_{\text{ads}})$ as the pair potential for particles in the bulk and adsorbed phases, respectively, where ϵ and λ (or ϵ_{ads} and λ_{ads}) are parameters that describe the energy depth and the range of the potential for the bulk and adsorbed particles, respectively.

Due to the presence of the wall, the fluid particle density, ρ , will be a function of z . To describe the amount of adsorbed particles the coverage Γ is introduced and defined as

$$\Gamma = \int_0^\infty dz [\rho(z) - \rho_b], \quad (3)$$

where ρ_b is the density of bulk particles, i.e., $\rho(z \rightarrow \infty)$. Since the length scale of the adsorbed fluid is defined by $\lambda_w \sigma$, we can rewrite Eq. (3) as

$$\Gamma = \int_0^{\lambda_w \sigma} dz \rho(z) - \rho_b \lambda_w \sigma, \quad (4)$$

where the integral of $\rho(z)$ in the right-hand term of Eq. (4) is the surface or adsorbed density,

$$\rho_{\text{ads}} = \int_0^{\lambda_w \sigma} dz \rho(z). \quad (5)$$

Equation (5) can be identified with a two-dimensional density, in such a way that the properties of the adsorbed fluid are represented as a 2D fluid.

Since in thermodynamic equilibrium, the chemical potentials of the adsorbed (μ_{ads}) and bulk (μ_b) phases must be equal for a given temperature T and bulk pressure P , ρ_{ads} can be obtained by solving the equation

$$\mu_{\text{ads}} = \mu_b. \quad (6)$$

The formal identification of the adsorbed fluid as a 2D system can be described as a decoupling of the x, y coordinates from the coordinate z for each adsorbed particle. In a similar way to the definition of the adsorbed density, we can define a 2D potential $\phi(x, y; \epsilon_{2D}, \lambda_{2D})$ from the actual pair potential $u_{pp}^{\text{ads}}(r; \epsilon_{\text{ads}}, \lambda_{\text{ads}})$ by integrating over the z coordinate,

$$\phi(x, y; \epsilon_{2D}, \lambda_{2D}) = \int_0^{\lambda_w \sigma} dz u_{pp}^{\text{ads}}(r; \epsilon_{\text{ads}}, \lambda_{\text{ads}}). \quad (7)$$

According to the definitions introduced previously, the partition function of the adsorbed fluid is given as

$$Z_{\text{ads}} = \frac{V_{\text{ads}}^N}{N! \Lambda^{3N}} Q_{\text{ads}}, \quad (8)$$

where V_{ads} is the volume containing the adsorbed fluid, Λ is the de Broglie thermal wavelength $\Lambda = h / (2\pi m k T)^{1/2}$ in

terms of Planck's constant h and the mass m of the particles, and Q_{ads} is the configurational partition function given by

$$Q_{\text{ads}} = \frac{1}{V_{\text{ads}}^N} \int dx^N dy^N dz^N e^{-\beta/2N(N-1)\phi(x,y) - Nu_{pw}(z)}. \quad (9)$$

By introducing the adsorption area S , we have that $V_{\text{ads}} = S\lambda_w\sigma$, and Q_{ads} can be rewritten as

$$Q_{\text{ads}} = Q_{1D}Q_{2D}, \quad (10)$$

where Q_{1D} and Q_{2D} are the one- and two-dimensional configurational partition functions, respectively, given by

$$Q_{1D} = \frac{1}{(\lambda_w\sigma)^N} \int dz^N e^{-\beta Nu_{pw}(z)} = \left[\frac{\int_0^{\lambda_w\sigma} dz e^{-\beta u_{pw}(z)}}{\lambda_w\sigma} \right]^N, \quad (11)$$

and

$$Q_{2D} = \frac{1}{S^N} \int d^N x d^N y e^{-\beta/2N(N-1)\phi(x,y)}. \quad (12)$$

The configurational partition function Q_{1D} in Eq. (11) can be evaluated using the mean-value theorem, i.e.,

$$\int_0^{\lambda_w\sigma} dz e^{-\beta u_{pw}(z)} = \lambda_w\sigma e^{-\beta u_{pw}(z^*)}, \quad (13)$$

where z^* is the value of the coordinate z that guarantees the mean value of the Boltzmann factor. In this way we obtain a simple result for Q_{1D} ,

$$Q_{1D} = e^{-N\beta u_{pw}(z^*)}, \quad (14)$$

and the final expression for the partition function given in Eq. (8) becomes

$$Z_{\text{ads}} = \frac{S^N}{N!\Lambda^{2N}} + \ln Q_{2D} + \left[\frac{\lambda_w\sigma}{\Lambda} \right]^N - N\beta u_{pw}(z^*). \quad (15)$$

Applying the standard relation $A = -kT \ln Z$, the Helmholtz free energy of the adsorbed fluid is given by

$$\frac{A_{\text{ads}}}{NkT} = \frac{A_{2D}}{NkT} - \ln \left(\frac{\lambda_w\sigma}{\Lambda} \right) + \beta u_{pw}(z^*), \quad (16)$$

where A_{2D} is the Helmholtz free energy of a two-dimensional fluid interacting via the potential $\phi(x,y)$, which can be described by perturbation theory,

$$\frac{A_{2D}}{NkT} = \ln(\rho_{\text{ads}}\Lambda^2) + \frac{A_{\text{HD}}}{NkT} + \beta a_1^{2D} + \beta^2 a_2^{2D}. \quad (17)$$

Here A_{HD} is the excess Helmholtz free energy for a fluid of hard disks, $\beta = 1/kT$, and a_1^{2D} and a_2^{2D} are the first two terms of the perturbation expansion in 2D. It is also relevant to stress that the expression given for Q_{1D} is exact, and this information appears in Eq. (16) as an external field that essentially can be used to define the energy parameter of the wall, ϵ_w . For the simple case where the wall-particle interaction is given by a square-well interaction of range $\lambda_w\sigma$ and energy depth ϵ_w , we have that $u_{pw}(z^*) = -\epsilon_w$.

For the bulk fluid, we consider an analogous perturbation expression,

$$\frac{A_{3D}}{NkT} = \ln(\rho_b\Lambda^3) + \frac{A_{\text{HS}}}{NkT} + \beta a_1 + \beta^2 a_2. \quad (18)$$

Obtaining the chemical potentials μ_{ads} and μ_b from Eqs. (16) and (18), we can rewrite Eq. (6) in the following way;

$$\mu_{3D} = \mu_{2D} + \mu_w, \quad (19)$$

where μ_{3D} and μ_{2D} are the chemical potentials for 3D and 2D fluids, respectively, and μ_w is the contribution to the chemical potential due to the wall,

$$\beta\mu_w = -\ln(\lambda_w) + \beta u_{pw}(z^*). \quad (20)$$

Before finishing this section, it is important to note that the method presented here can be extended to describe adsorption phenomena where the particle-particle and wall-particle interactions are described by discontinuous potentials of more general form than the square-well (SW) potential. A general theory for 3D discrete-potential fluids has been presented by Benavides and Gil-Villegas³⁷ and Vidales *et al.*³⁸ that can accurately describe the properties of Lennard-Jonessium systems, and can easily be extended to 2D fluids, using the approach presented here.

B. Adsorption of chain molecules

The theory presented in Sec. II A above is easily extended to the general case of adsorption of homonuclear and heteronuclear chain molecules,^{39,40} within the SAFT-VR framework.^{31,41} In the simplest case of homonuclear molecules, we consider that the fluid is formed by N molecules each composed of m spherical segments of diameter σ . We assume that the particle-particle and particle-wall interactions are described by square-well potentials. The thermodynamic equilibrium between the bulk and adsorbed fluid is obtained from the equality of the chemical potentials, as given by Eq. (19). The chemical potentials are derived from the SAFT-VR expressions for the Helmholtz free energies for 3D and 2D chain-molecule fluids. The 2D case has been developed recently and is reported elsewhere.⁴²

C. 3D and 2D SAFT-VR approach

The Helmholtz free energy for chain molecules in the SAFT-VR approach is written as separate terms, which account for the ideal, monomer, and chain contributions to the free energy,

$$\frac{A}{NkT} = \frac{A^{\text{ideal}}}{NkT} + \frac{A^{\text{mono}}}{NkT} + \frac{A^{\text{chain}}}{NkT}. \quad (21)$$

Here we summarize the main expressions for these quantities, in three and two dimensions. Detailed information about the 3D expressions can be found in Ref. 31 and for the 2D case in Appendix.

1. Ideal contribution

$$\frac{A_{3D}^{\text{ideal}}}{NkT} = \ln(\rho_b\Lambda^3) \quad (22)$$

$$\frac{A_{2D}^{\text{ideal}}}{NkT} = \ln(\rho_{\text{ads}}\Lambda^2), \quad (23)$$

where Λ is the thermal de Broglie wavelength.

2. Monomer contribution

$$\frac{A_{3D}^{\text{mono}}}{NkT} = m \frac{A_{3D}}{N_s kT}, \quad (24)$$

$$\frac{A_{2D}^{\text{mono}}}{NkT} = m \frac{A_{2D}}{N_s kT}, \quad (25)$$

where A_{3D} and A_{2D} are the Helmholtz free energies for 3D and 2D monomeric fluids, respectively, i.e., systems composed by N_s spheres interacting via a SW potential. These terms are obtained from perturbation theory, as expressed by Eqs. (18) and (17).

3. Chain contribution

$$\frac{A_{3D}^{\text{chain}}}{NkT} = -(m-1) \ln y^{3\text{DSW}}(\sigma), \quad (26)$$

$$\frac{A_{2D}^{\text{chain}}}{NkT} = -(m-1) \ln y^{2\text{DSW}}(\sigma), \quad (27)$$

where $y^{2\text{DSW}}$ and $y^{3\text{DSW}}$ are the 2D and 3D background correlation functions that are obtained from the respective radial distribution function using the well-known relationship $y(r) = g(r)e^{\beta u(r)}$. Following the SAFT-VR procedure, $g(r)$ is obtained also from a high temperature perturbation expansion approach,

$$g^{3\text{DSW}}(\sigma) = g^{\text{HS}}(\sigma) + \beta \epsilon g_1^{3\text{D}}(\sigma), \quad (28)$$

$$g^{2\text{DSW}}(\sigma) = g^{\text{HD}}(\sigma) + \beta \epsilon g_1^{2\text{D}}(\sigma). \quad (29)$$

III. COMPUTER SIMULATIONS

In order to validate the new theoretical approach and determine the conditions under which the approximations developed in this work are valid, computer simulations have been performed to calculate the adsorption isotherms for a monomeric SW fluid confined between planar walls. Simulations were performed using the Gibbs ensemble Monte Carlo simulation method for inhomogeneous fluids (GEMC-IFs),⁴³ which provides structural and thermodynamic properties for bulk and confined fluids. In the GEMC-IF method the bulk and confined fluids are simulated in two different boxes. Using a Monte Carlo procedure, particles are moved through independent displacement of the particles in both boxes and an interchange of particles between boxes, keeping the total number of molecules constant. A cycle is defined by N particle displacements and a fixed number of particle interchanges. The number of attempted particle interchanges was controlled so that above 5% of the molecules are exchanged each cycle. The results presented here were obtained using 1728 particles and 40 000 cycles for equilibration, with another 40 000 for av-

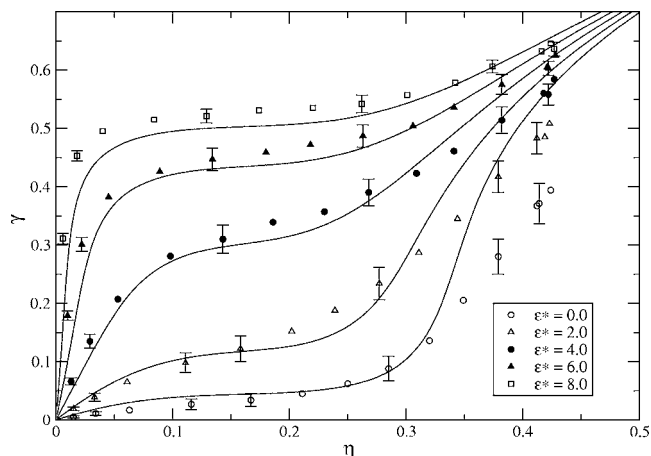


FIG. 1. Adsorption isotherms for a monomeric SW fluid confined between planar walls at $T^* = 1.5$. The wall-particle interaction is described by a SW potential with depth ϵ_w and range λ_w . Symbols are 2D packing fractions obtained from density profiles simulated with the Gibbs ensemble Monte Carlo technique for inhomogeneous fluids. The particle-particle SW range is $\lambda = 1.5$, whereas the particle-wall SW range is $\lambda_w = 0.2453$. Different isotherms are reported, according to the value of $\epsilon^* = \epsilon_w/\epsilon$. Lines correspond to the theoretical predictions obtained from the SAFT-VR approach for bulk (3D) and adsorbed (2D) fluids. Symbols are GEMC-IF results.

eraging. All simulations were performed for a fixed distance of 15σ between the walls. Additional details of the procedure followed are described in Refs. 44 and 45.

From the simulated density profiles $\rho(z)$, the bulk and confined packing fractions were obtained as $\eta = \pi \rho_b \sigma^3/6$ and $\gamma = \pi \rho_{\text{ads}} \sigma^2/4$, respectively. The adsorbed density was then evaluated through Eq. (5), viz.,

$$\rho_{\text{ads}} = \int_0^{\lambda_w \sigma} \rho(z) dz. \quad (30)$$

IV. RESULTS

A comparison of the theoretical predictions and simulation data for the adsorption isotherms of SW monomeric fluids with range $\lambda = 1.5$ is presented in Fig. 1. Adsorption isotherms are given for five different wall-particle interactions, according to the energy depth of the SW fluid, namely, $\epsilon^* = \epsilon_w/\epsilon = 0.0, 2.0, 4.0, 6.0,$ and 8.0 . Very good agreement between the theoretical predictions and simulation data is observed for $\eta \leq 0.3$ if $\epsilon^* \leq 2.0$, and for $\eta \leq 0.4$ if $\epsilon^* > 2.0$. Deviations are significant in the high bulk-density and low wall-energy region. In order to visualize the behavior represented by the adsorption isotherms, in Fig. 2 we present a series of snapshots for a low ($\epsilon^* = 2.0$) and a high value ($\epsilon^* = 8.0$) of the wall-particle energy. Packing fractions at approximately the same value for the two systems chosen were selected. These values were $\eta = 0.0329, 0.0606, 0.1583,$ and 0.3789 when $\epsilon^* = 2.0$, and $\eta = 0.0179, 0.0400, 0.1289,$ and 0.3737 when $\epsilon^* = 8.0$. From these snapshots we can see that for the highest value of ϵ^* well defined layers of the adsorbed fluid are observed for all densities. In the case of the lowest energy, the layers are not as well formed. Therefore we can conclude that the quasi-2D approach used here to describe the adsorbed fluid is a valid approximation when the formation of layers is enhanced. This result suggests that the par-

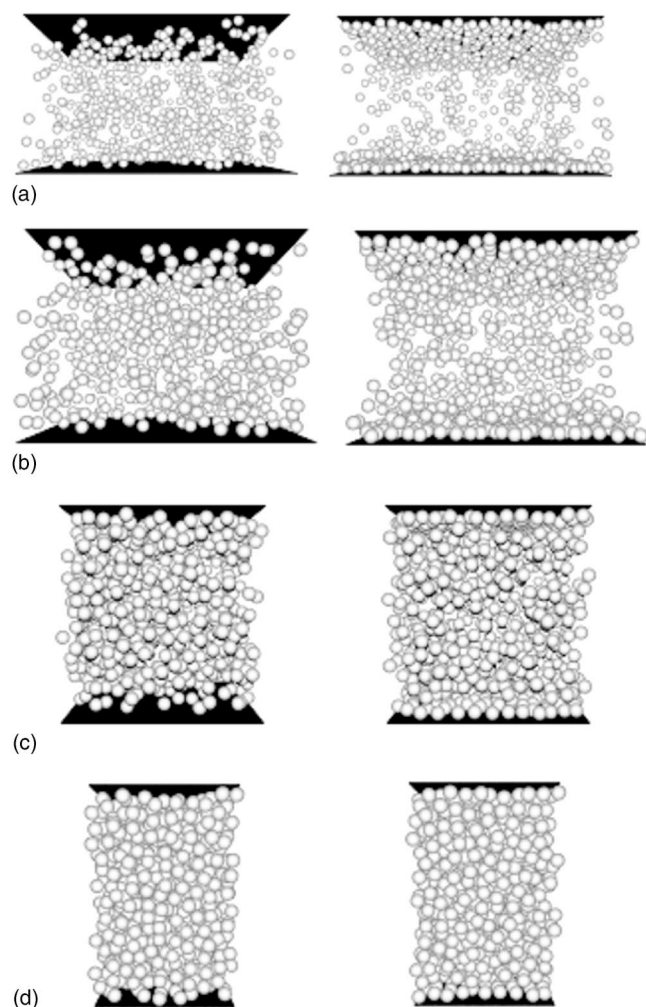


FIG. 2. Snapshots of configurations from simulations reported in Fig. 1. Left-hand-side images correspond to $\epsilon^* = \epsilon_w / \epsilon = 2.0$ with bulk fluid packing fractions η given as (a) 0.0329, (b) 0.0606, (c) 0.1583, and (d) 0.3789. Right-hand-side images correspond to $\epsilon^* = 8.0$ with η : (a) 0.0179, (b) 0.0400, (c) 0.1289, and (d) 0.3737.

ticles within the layers behave effectively as a 2D system, and the effect is more noticeable as ϵ^* increases. As we will discuss next, experimental values of adsorption energies correspond to high values of ϵ^* .

Having validated the new theoretical approach we now test the application of our theory to real substances. In particular, we have studied the adsorption of methane and nitrogen on dry activated carbon. In Table I the molecular parameters used to describe the bulk and adsorbed fluids are reported. The bulk fluids were modeled using parameters previously reported for methane and nitrogen within the SAFT-VR approach.^{31,46,47} As we can see from Table I, methane is represented by a monomeric fluid ($m=1$) and nitrogen as a nonspherical molecule ($m=1.33$), in both the

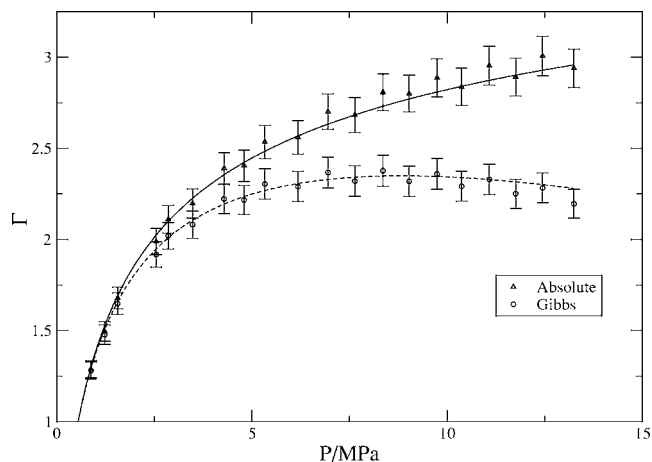


FIG. 3. Adsorption isotherms for methane adsorbed on dry activated carbon at 318.2 K. Gibbs and absolute adsorption isotherms are reported scaled with their respective values at 0.55 MPa. Theoretical correlations are represented as lines and the experimental data (Ref. 48) as symbols.

bulk and adsorbed phases. The diameters of the spherical segments, σ , are also the same for bulk and adsorbed molecules, whereas the parameters of the SW attractive potentials are different. These differences are due to the influence of the substrate on the pair potential, as we have discussed before. According to the theoretical results derived by Sivanoglu and Pitzer³⁶ for a Lennard-Jones fluid, the energy well depth of the particle-particle potential in an adsorbed monolayer is reduced by 20%–40% from its bulk phase value. In our case, we selected a reduction factor of 20%, as reported in Table I for ϵ_{ads} for methane and nitrogen. Once ϵ_{ads} is selected in this way, the range λ_{ads} can be determined by reproducing the experimental ratio between the critical temperatures of the bulk (T_c^{bulk}) and adsorbed (T_c^{ads}) phases, i.e., $R_c = T_c^{\text{ads}} / T_c^{\text{bulk}}$. This ratio is known for the case of noble gases and methane adsorbed onto a graphite surface, $R_c \approx 0.4$. λ_{ads} was determined in order to reproduce this ratio with the parameter values for methane and nitrogen (i.e., m , σ , ϵ , λ , and ϵ_{ads}) as reported in Table I.

In Table I we also report the parameter values used for the wall-particle potential. A value of 0.8165 was used for the range λ_w and corresponds to the upper limit that can be used to describe monolayer adsorption according to mean-field criteria.³⁴ The energy parameter ϵ_w was fitted in order to reproduce the adsorption isotherm data.

In Figs. 3 and 4 we present results obtained for the adsorption isotherms of methane and nitrogen on dry activated carbon. Gibbs and absolute adsorption isotherms were obtained according to Eqs. (4) and (5), respectively, and compared with the experimental data reported by Sudibandriyo *et al.*⁴⁸ We can see that the agreement between the theoretical correlations and experimental data in both cases are very

TABLE I. Values of the molecular parameters used to describe methane and nitrogen adsorption on dry activated carbon.

| Substance | m | σ (Å) | λ | ϵ/k (K) | λ_{ads} | ϵ_{ads}/k (K) | λ_w | ϵ_w/ϵ |
|-----------|------|--------------|-----------|------------------|------------------------|-------------------------------|-------------|-----------------------|
| Methane | 1.0 | 3.670 | 1.444 | 168.8 | 1.2 | 133.1 | 0.8165 | 7.80 |
| Nitrogen | 1.33 | 3.159 | 1.550 | 81.4851 | 1.4737 | 65.188 | 0.8165 | 10.0 |

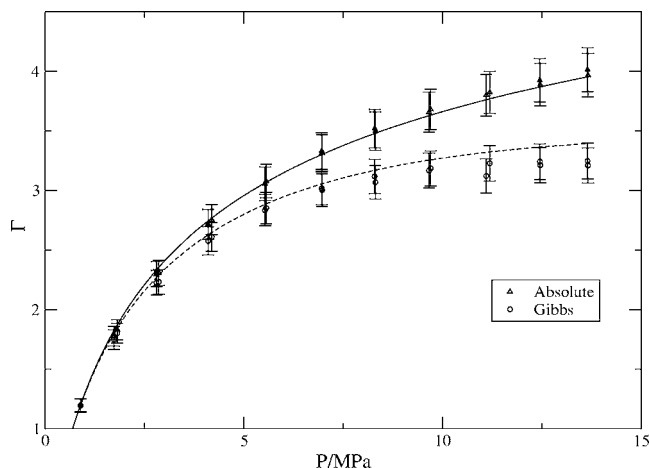


FIG. 4. Adsorption isotherms for nitrogen adsorbed on dry activated carbon at 318.2 K. Gibbs and absolute adsorption isotherms are reported scaled with their respective values at 0.69 MPa. Theoretical correlations are represented as lines and the experimental data (Ref. 48) as symbols.

good. The values obtained for ϵ^* of 7.80 for methane and 10.0 for nitrogen were determined from a best fit to the experimental data. It is important to note here that ϵ^* could be estimated from experimental values of the adsorbate energies U_w , if this is known. For example, for krypton adsorbed on graphite $U_w = 11.72$ kJ/mol (Ref. 49) and would correspond to $\epsilon^* = 8.168$,³⁴ which is of comparable magnitude to the values used in this work.

V. CONCLUSIONS

In this study we have extended the scope of the SAFT-VR approach to model adsorption isotherms for non-associating chain fluids. Using a quasi-2D approach, we have shown that the new theory can accurately describe computer simulation results for a number of model systems. In addition, we have shown that the new approach can be used to reproduce accurately the adsorption of real substances using molecular parameters obtained independently for modeling bulk fluids with the SAFT-VR equation. This work represents the first extension and application of the SAFT-VR method to model confined fluids. In future work, issues such as the heterogeneity of the confining surfaces as well as the size of the pores will be considered.

ACKNOWLEDGMENTS

Two of the authors (A.M. and M.C.) acknowledge Ph.D. scholarships from CONACYT. This work was supported under CONACYT Grant Nos. 2003-C03-42439/A-1 and 41678-F. Another author (C.M.C.) acknowledges financial support from the National Science Foundation under Grant No. CTS-0453229.

APPENDIX: 3D AND 2D SAFT-VR EXPRESSIONS

In this appendix we report detailed expressions required to apply the theoretical approach developed in this article. The reader is directed to Refs. 31 and 42 for additional details.

1. SAFT-VR 3D

The hard-sphere Helmholtz free energy is given by the Carnahan-Starling equation,⁵⁰

$$\frac{A_{\text{HS}}}{N_s kT} = \frac{4\eta - 3\eta^2}{(1-\eta)^2}. \quad (\text{A1})$$

The corresponding contact value of the radial distribution function, required to evaluate the chain contribution to the free energy, is given by

$$g^{\text{HS}}(\sigma, \eta) = \frac{1 - \eta/2}{(1 - \eta)^2}. \quad (\text{A2})$$

The first-order perturbation term $a_1^{3\text{D}}$ is given by

$$a_1^{3\text{D}} = -4\eta\epsilon(\lambda^3 - 1)g^{\text{HS}}(\sigma, \eta_{\text{eff}}), \quad (\text{A3})$$

where the contact value of the HS radial distribution function is used again but evaluated at an effective packing fraction, η_{eff} , given by

$$\eta_{\text{eff}} = c_1\eta + c_2\eta^2 + c_3\eta^3, \quad (\text{A4})$$

where c_1 , c_2 , and c_3 are quadratic expressions of the range λ ,

$$c_1 = 2.25855 - 1.50349\lambda + 0.249434\lambda^2, \quad (\text{A5})$$

$$c_2 = -0.669270 + 1.40049\lambda - 0.827739\lambda^2, \quad (\text{A6})$$

$$c_3 = 10.1576 - 15.0427\lambda + 5.30827\lambda^2. \quad (\text{A7})$$

The second-order perturbation term $a_2^{3\text{D}}$ is obtained from the local compressibility approximation,

$$a_2^{3\text{D}} = \frac{1}{2}\epsilon \frac{(1-\eta)^4}{1+4\eta+4\eta^2} \eta \frac{\partial a_1^{3\text{D}}}{\partial \eta}. \quad (\text{A8})$$

The first-order perturbation term of the contact value of the SW radial distribution function is derived from a self-consistent procedure that enforces the equality of the pressure obtained from the Helmholtz free energy and the pressure obtained from the Clausius virial theorem,

$$g_1^{3\text{D}}(\sigma) = \frac{1}{4}\beta \left[\frac{\partial a_1^{3\text{D}}}{\partial \eta} - \frac{\lambda}{3\eta} \frac{\partial a_1^{3\text{D}}}{\partial \lambda} \right]. \quad (\text{A9})$$

2. SAFT-VR-2D

The corresponding expressions for the 2D version of the SAFT-VR approach follow the same structure as in the 3D case.

The Helmholtz free energy for a hard-disk fluid is obtained from the Henderson equation,⁵¹

$$\frac{A^{\text{HD}}}{N_s kT} = \frac{9\gamma}{8(1-\gamma)} - \frac{7}{8} \ln(1-\gamma), \quad (\text{A10})$$

and the corresponding contact value of the radial distribution function g^{HD} is given by

$$g^{\text{HD}}(\sigma) = \frac{1 - 7\gamma/16}{(1-\gamma)^2}. \quad (\text{A11})$$

The first order perturbation term of the Helmholtz free energy is given by

$$a_1^{2D} = -2\gamma\epsilon(\lambda^2 - 1)g^{\text{HD}}(\sigma, \gamma_{\text{eff}}), \quad (\text{A12})$$

where, as in the 3D case, the radial distribution function at contact, g^{HD} , is evaluated with an effective packing fraction γ_{eff} given by

$$\gamma_{\text{eff}} = d_1\gamma + d_2\gamma^2, \quad (\text{A13})$$

where

$$d_1 = 1.4215 - 0.405625\lambda - 0.386981\lambda^2, \quad (\text{A14})$$

and

$$d_2 = 1.5582 - 1.89768\lambda + 0.405215\lambda^2. \quad (\text{A15})$$

The second-order term is given by the local compressibility approximation result,

$$a_2^{2D} = \frac{1}{2}\epsilon \frac{(1-\gamma)^3}{1+\gamma+0.375\gamma^2-0.125\gamma^3} \gamma \frac{\partial a_1^{2D}}{\partial \gamma}. \quad (\text{A16})$$

Finally, $g_1^{2D}(\sigma)$ is given by the self-consistent expression,

$$g_1^{2D}(\sigma) = \frac{1}{2\epsilon} \left[\frac{\partial a_1^{2D}}{\partial \gamma} - \frac{\lambda}{2\gamma} \frac{\partial a_1^{2D}}{\partial \lambda} \right]. \quad (\text{A17})$$

¹E. F. Vansant, *Stud. Surf. Sci. Catal.* **120B**, 381 (1998).

²Y. I. Tarasevich, *Stud. Surf. Sci. Catal.* **120B**, 659 (1998).

³A. Daehler, G. W. Stevens, and A. J. O'Connor, in *Nanoporous Materials, Science and Engineering*, Series on Chemical Engineering, edited by G. Q. Lu and X. S. Zhao (Imperial College Press, London, 2004), p. 812.

⁴L. D. Gelb, K. E. Gubbins, R. Radhakrishnan, and M. Sliwinski-Bartowiak, *Rep. Prog. Phys.* **62**, 1573 (1999).

⁵R. Evans, in *Fundamentals of Inhomogeneous Fluids*, edited by D. Henderson (Dekker, New York, 1992), p. 85.

⁶C. Ebner, W. F. Saam, and D. Stroud, *Phys. Rev. A* **14**, 2264 (1976).

⁷C. Ebner and W. F. Saam, *Phys. Rev. Lett.* **38**, 1486 (1977).

⁸W. F. Saam and C. Ebner, *Phys. Rev. A* **17**, 1768 (1978).

⁹D. E. Sullivan and M. M. Telo da Gama, in *Fluid Interfacial Phenomena*, edited by C. A. Croxton (Wiley, New York, 1986), p. 45.

¹⁰P. I. Ravikovitch, A. Vishnyakov, and A. V. Neimark, *Phys. Rev. E* **64**, 011602 (2001).

¹¹R. Evans, U. M. B. Marconi, and P. Tarazona, *J. Chem. Phys.* **84**, 2376 (1986).

¹²A. V. Neimark, P. I. Ravikovitch, and A. Vishnyakov, *J. Phys.: Condens. Matter* **1**, 347 (2003).

¹³W. G. Chapman, K. E. Gubbins, G. Jackson, and M. Radosz, *Fluid Phase Equilib.* **52**, 31 (1989).

¹⁴W. G. Chapman, K. E. Gubbins, G. Jackson, and M. Radosz, *Ind. Eng. Chem. Res.* **29**, 1709 (1990).

¹⁵M. S. Wertheim, *J. Stat. Phys.* **35**, 19 (1984).

¹⁶M. S. Wertheim, *J. Stat. Phys.* **35**, 35 (1984).

¹⁷M. S. Wertheim, *J. Stat. Phys.* **42**, 459 (1986).

¹⁸M. S. Wertheim, *J. Stat. Phys.* **42**, 477 (1986).

¹⁹M. S. Wertheim, *J. Chem. Phys.* **85**, 2929 (1986).

²⁰M. S. Wertheim, *J. Chem. Phys.* **87**, 7323 (1987).

²¹G. J. Gloor, F. J. Blas, E. M. del Río, E. de Miguel, and G. Jackson, *Fluid Phase Equilib.* **194–197**, 521 (2002).

²²C. J. Segura and W. G. Chapman, *Mol. Phys.* **86**, 415 (1995).

²³C. J. Segura, W. G. Chapman, and K. P. Shukla, *Mol. Phys.* **90**, 759 (1997).

²⁴C. J. Segura, J. Zhang, and W. G. Chapman, *Mol. Phys.* **99**, 1 (2001).

²⁵A. Patrykiewicz and S. Sokolowski, *J. Phys. Chem. B* **103**, 4466 (1999).

²⁶A. Huerta, O. Pizio, and S. Sokolowski, *J. Chem. Phys.* **112**, 4286 (2000).

²⁷E. A. Muller and K. E. Gubbins, in *Equations of State for Fluids and Fluids Mixtures*, edited by J. V. Sengers, R. F. Kayser, C. J. Peters, and H. J. White (Elsevier, Amsterdam, 2000), p. 435.

²⁸E. A. Muller and K. E. Gubbins, *Ind. Eng. Chem. Res.* **40**, 2193 (2001).

²⁹I. G. Economou, *Ind. Eng. Chem. Res.* **41**, 953 (2002).

³⁰P. Paricaud, A. Galindo, and G. Jackson, *Fluid Phase Equilib.* **194–197**, 87 (2002).

³¹A. Gil-Villegas, A. Galindo, P. J. Whitehead, S. J. Mills, G. Jackson, and A. N. Burgess, *J. Chem. Phys.* **106**, 4168 (1997).

³²J. H. de Boer, *The Dynamical Character of Adsorption* (Oxford University Press, Oxford, 1953).

³³J. G. Dash, *Films on Solid Surfaces* (Academic, New York, 1975).

³⁴F. del Río and A. Gil-Villegas, *J. Phys. Chem.* **95**, 788 (1991).

³⁵R. A. Pierotti and H. E. Thomas, *Surface and Colloid Sciences* (Wiley-Interscience, New York, 1971).

³⁶O. Sinanoglu and K. S. Pitzer, *J. Chem. Phys.* **32**, 1279 (1960).

³⁷A. L. Benavides and A. Gil-Villegas, *Mol. Phys.* **97**, 1225 (1999).

³⁸A. Vidales, A. L. Benavides, and A. Gil-Villegas, *Mol. Phys.* **99**, 703 (2001).

³⁹C. McCabe, A. Gil-Villegas, G. Jackson, and F. del Río, *Mol. Phys.* **97**, 551 (1999).

⁴⁰Y. Peng, H. Zhao, and C. McCabe, *Mol. Phys.* **104**, 571 (2006).

⁴¹A. Galindo, L. A. Davies, A. Gil-Villegas, and G. Jackson, *Mol. Phys.* **93**, 241 (1998).

⁴²M. Castro, J. Huang, V. Pérez, C. McCabe, and A. Gil-Villegas, *Mol. Phys.* (in preparation).

⁴³A. Z. Panagiotopoulos, *Mol. Phys.* **62**, 701 (1987).

⁴⁴L. A. del Pino, A. L. Benavides, and A. Gil-Villegas, *Mol. Simul.* **29**, 345 (2003).

⁴⁵A. L. Benavides, L. A. del Pino, A. Gil-Villegas, and F. Sastre, *J. Chem. Phys.* **125**, 204715 (2006).

⁴⁶C. McCabe, A. Galindo, A. Gil-Villegas, and G. Jackson, *Int. J. Thermophys.* **19**, 1551 (1998).

⁴⁷H. Zhao, P. Morgado, A. Gil-Villegas, and C. McCabe, *J. Phys. Chem. B* **110**, 24083 (2006).

⁴⁸M. Sudibandriyo, Z. Pan, J. E. Fitzgerald, R. L. Robinson, Jr., and A. M. Gasem, *Langmuir* **345**, 5323 (2003).

⁴⁹S. Ross and J. P. Oliver, *On Physical Adsorption* (Interscience, New York, 1964), p. 234.

⁵⁰N. F. Carnahan and K. E. Starling, *J. Chem. Phys.* **51**, 635 (1969).

⁵¹D. Henderson, *Mol. Phys.* **30**, 971 (1975).